Letter

Cation Engineering for Resonant Energy Level Alignment in Two-Dimensional Lead Halide Perovskites

Nadège Marchal, Edoardo Mosconi,* Gonzalo García-Espejo, Tahani M. Almutairi, Claudio Quarti, David Beljonne, and Filippo De Angelis*

Read Online

ACCESS | Metrics & More | Article Recommendations | Supporting Information

ABSTRACT: Low-dimensional metal halide perovskites are being intensively investigated because of their higher stability and chemical versatility in comparison to their 3D counterparts. Unfortunately, this comes at the expense of the electronic and charge transport properties, limited by the reduced perovskite dimensionality. Cation engineering can be envisaged as a solution to tune and possibly further improve the material's optoelectronic properties. In this work, we screen and design new electronically active A-site cations that can promote charge transport across the inorganic layers. We show that hybridization of the valence band electronic states of the perovskite inorganic sublattice and the highest occupied molecular orbitals of the A-site organic cations can be tuned to exhibit a variety of optoelectronic properties. A significant interplay of A-cation size, electronic structure, and steric constraints is revealed, suggesting intriguing means of further tuning the 2D perovskite electronic structure toward achieving stable and efficient solar cell devices.
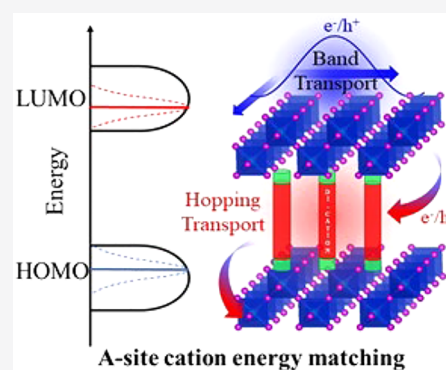
Metal halide perovskites (MHPs) have been in the spotlight for a decade in the world of semiconductors because of their impressive properties for optoelectronic applications, including, but not limited to, photovoltaics.[1−7] Within the general AMX$_3$ stoichiometry typical of corner-sharing three-dimensional (3D) perovskites, the A-site cation is placed into the cuboctahedral cavities created by the inorganic framework (M = Pb, Sn, Ge; X = I, Br, Cl). These 3D materials gained quickly in interest because of their easy solution-based synthesis and their impressive optoelectronic properties, which led to a certified solar cell efficiency exceeding 25%[8] in single-junction thin-film devices. These 3D materials suffer, however, from severe degradation issues,[9] related to light-, environment-, and thermal-induced instabilities.[10,11]

As an alternative to 3D materials, lower-dimensional perovskites, obtained by adjusting the precursor composition and introducing larger A-site cations, have gained considerable interest as it was realized that the ensuing layered structures usually exhibit increased stability compared to their 3D counterparts. Also, these low-dimensional perovskites offer a huge increase in terms of chemical flexibility, not being limited in the selection of A-site cations by the size of the cavities created by the inorganic network.[10] Typical two-dimensional (2D) MHPs are composed of organic cations, mainly alkyl chains of different size, ended by an ammonium group binding the inorganic sublattice (Scheme 1). Depending on the nature and charge of the A-site cations, (100) or (110) stacking of the inorganic layers can be attained (Scheme 1), with typical A$_2$MX$_4$ and AMX$_4$ stoichiometry obtained by mono- and

dications, respectively, further expanding the structural and chemical portfolio of 2D perovskites.

In-depth investigations on these materials have provided many clarifications about the effects of dielectric confinement[11−13] and structural changes[14,15] on their optoelectronic properties.[18] These works have also highlighted, however, the main flaw of low-dimensional hybrid perovskites: the increased stability and chemical flexibility come at the expense of the optoelectronic properties of these materials. Introduction of electronically inert/insulating organic spacers spacing organic cations prevents the out-of-plane charge transport (i.e., in the stacking direction; Scheme 1), and it generally increases the material's band gap by virtue of quantum and dielectric confinement.[19,20] A main challenge is thus to combine the stability advantages of 2D perovskites with improved electronic properties, developing functional materials with optoelectronic properties approaching those of the 3D counterparts. Mixed dimensionality systems, such as Ruddlesden−Popper or Dion−Jacobson perovskites, composed of 2D and 3D domains alternated along one crystal axis, have been investigated in this context.[16−18] Mixing 2D and 3D perovskites in a proper way could afford a suitable combination of the impressive
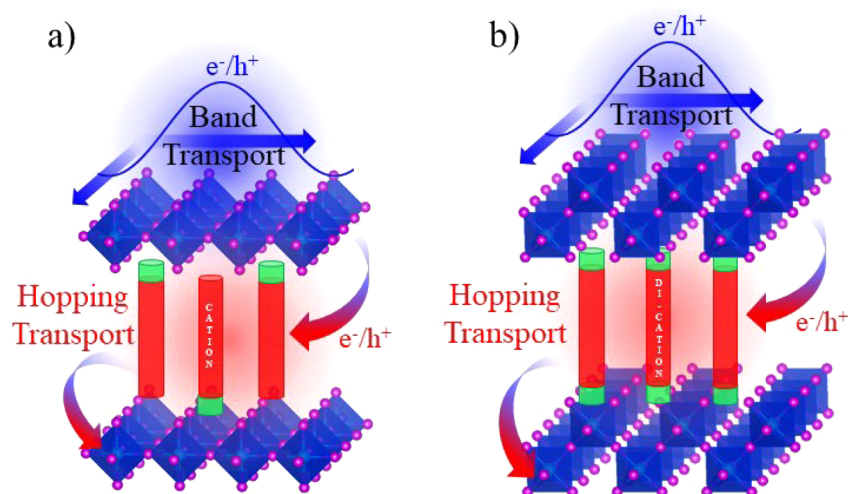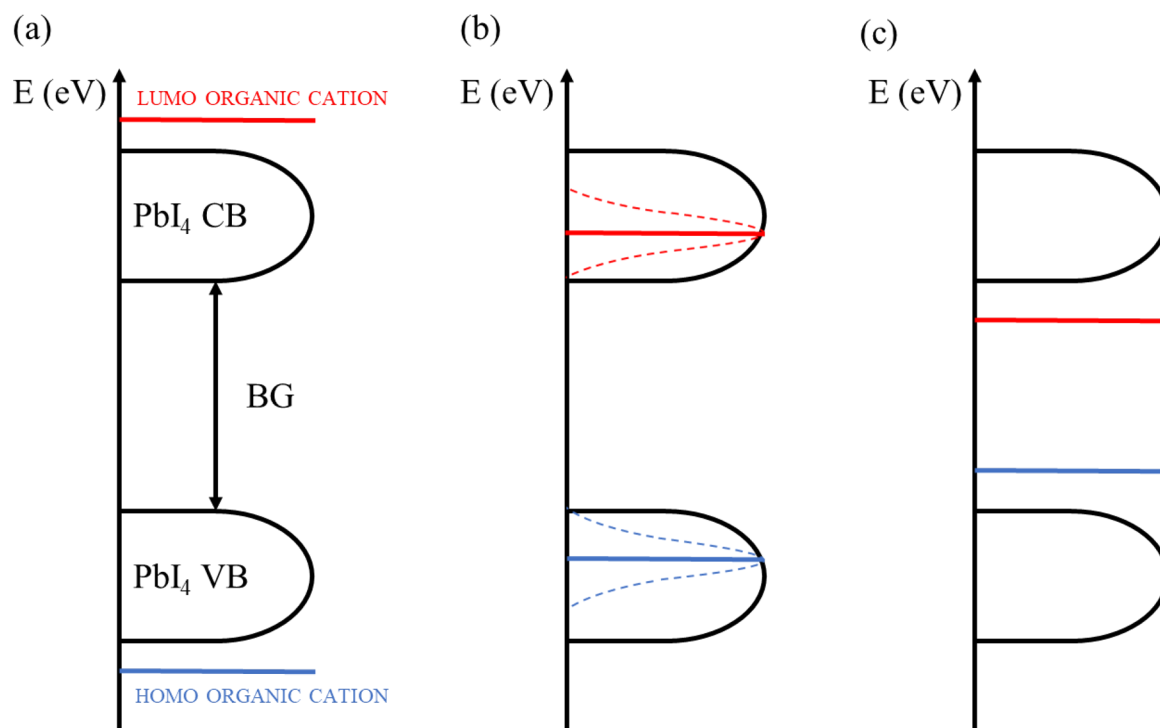
Scheme 1. Scheme of Crystal Structures of Generic 2D Perovskites with A-Site Cation (Red Cylinders with Green Positive Terminations) That Separate the Inorganic Layers (Blue Octahedra)[a]

[a](a) (100) $n = 1$ (usually with monocations); (b) (110) $n = 1$ (usually with dications).

Scheme 2. Schematic Representation of the Different Types of Energy Level Alignment between the A-Site Organic Cations and the Inorganic Part[a]

[a](a) The LUMO (HOMO) of the organic cation is higher (lower) in energy according to the CB (VB) of the inorganic part (like in the case of saturated cations). (b) The LUMO (HOMO) of the organic cation is aligned to the CB (VB) of the inorganic part. (c) The LUMO (HOMO) is integrated inside the BG of the perovskite. The dashed lines represent the potential broadening of the energy levels of the isolated cation upon interaction with the inorganic lattice.

optoelectronic properties from the 3D domains, with a wide range radiation absorption and good transport, and the stability provided by the 2D domains.[27] It appears, however, that charge carriers remain confined in the inorganic layers because of the electric isolation of the organic saturated cation introduced by the 2D domains. To find a solution to this problem, Tsai et al.[19] showed 2D perovskite films in which the inorganic layers show a preferential out-of-plane alignment

conformal to solar cell contacts, achieving >12% power conversion efficiency.

A different and possibly complementary approach is to use functionalized A-site cations,[20−24] which could endow the organic layers with specific optoelectronic properties. Borrowing from wide experience in organic electronics, these molecules should be composed of aromatic rings, conjugated multiple bonds, or charge-transfer complexes, instead of

saturated alkyl chains. In principle, these molecules are capable of transporting charges and electronic excitations between the inorganic layers, while still blocking ionic diffusion and environmental hazards. The way the organic cations would contribute to transport properties strongly depends on the energy level alignment at the organic−inorganic interface.

The mixed band and hopping transport schematically shown in Scheme 1 can be expected in the case where the frontier organic molecular orbitals are lying within the inorganic semiconducting bandgap (type I heterojunction), see Scheme 2c, while fully saturated inert organic cations usually lead to the situation displayed in Scheme 2a. Scenarios a and c in Scheme 2 are not ideal, as in 2a the organic cations act as insulating layers, while in 2b transient localization of the charges on the organic translates into the formation of "heavy" vibrationally dressed and weakly mobile molecular polarons. The target of a proper design strategy should aim at the situation depicted in Scheme 2b, where a proper alignment of the energy levels combined with a strong electronic coupling between the organic cations and the lead halide network results in improved hopping and band transport. In this sense we should be looking for organic cations endowed with either or both HOMO and LUMO levels properly aligned with the VB or CB edges, respectively, and that may be properly hybridized with the inorganic sublattice thanks to significant wave function overlap.

To this aim, we investigate the electronic structure of prototypical 2D perovskite inorganic scaffolds intercalated by selected A-site cations, which we computationally screened among a vast data set of mono- and dications in search of energy alignment and electronic interactions leading to the resonant energy level alignment and significant electronic coupling, reaching the target of Scheme 2b. The main purpose of this study is to identify an organic cation showing the HOMO and LUMO energy levels aligned to the VB and CB edges of the inorganic states (Scheme 2b), and at the same time, the organic molecules have to show a geometry and steric encumbrance suitable to be adapted in the inorganic network. On the basis of a subset of computationally screened selected cations we investigate typical (100) and (110) perovskites (Scheme 1), showing known A-site cations against the novel proposed ones. Our analysis discloses the fundamental requisites needed to obtain the long sought vertical charge transport in 2D perovskites, further expanding their application potential, and highlights a synthetically feasible new perovskite which could show the desired vertical transport properties.

We start our analysis by investigating the electronic structure of two prototypical 2D compounds with ⟨110⟩- and ⟨100⟩-orientations, namely, EDBEPbI$_4$ and NBT$_2$PbI$_4$ [EDBE = 2,2-(ethylenedioxy)bis(ethylammonium), NBT = n-butylammonium][25] (see calculated crystal structures in Figure 1).

To obtain accurate electronic structure and alignment of inorganic and organic sublevels we resort to high-level HSE06-SOC calculations. We compare the partial density of states (PDOS) of EDBEPbI$_4$ and NBT$_2$PbI$_4$ in Figure 2. In both cases the organic cations show negligible contribution to the valence band edge (VBE) though stronger organic/inorganic coupling is calculated in EDBEPbI$_4$. We recall that the electronic coupling of the organic cation interacting with the inorganic sublattice can be estimated by the broadening of the energy level of the isolated cation upon interaction.[26] To estimate this broadening, we compared the PDOS of the perovskite structures with those of the noninteracting organic
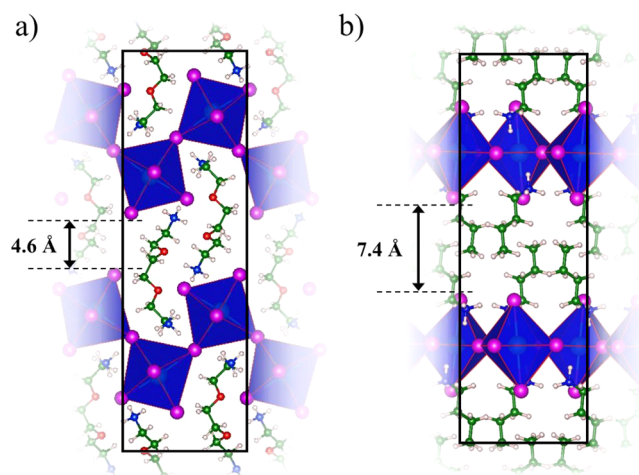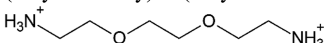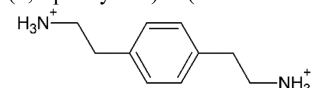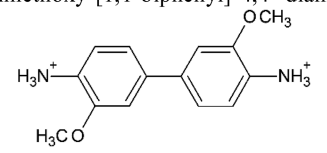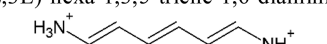

Figure 1. Optimized geometry structures of (a) ⟨110⟩-oriented EDBEPbI$_4$ and (b) ⟨100⟩-oriented NBT$_2$PbI$_4$ perovskite. The distance between the inorganic layers is also reported in angstroms.
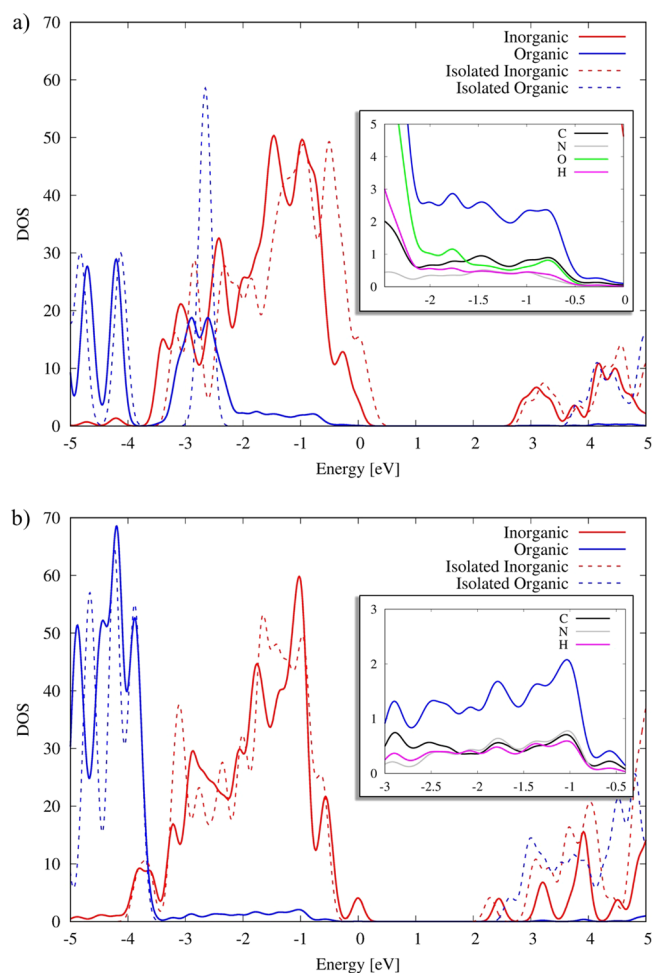
Figure 2. Partial density of states (PDOS) of (a) EDBEPbI$_4$ and (b) NBT$_2$PbI$_4$ calculated at the HSE06-SOC level. The red line represents the inorganic part, whereas the blue line represents the contribution of the organic cations. The full lines represent the PDOS of the complete system (organic and inorganic parts interacting), and the dashed lines represent the DOS of organic and inorganic parts calculated separated. The insets show the contribution of the atomic species associated with the organic molecules.

Table 1. Calculated HOMO and LUMO Energies (eV) in Polar Solvent for the Investigated Molecules along with the N−N Distance in Angstroms[a]

	A-site di-cations	H	L	N-N dist.	I-I dist.	Vol. $Å^3$
1	2,2-(ethylenedioxy)bis(ethylammonium)) $H_3N^+ \diagdown\diagup O \diagdown\diagup O \diagdown NH_3^+$	-7.83	0.64	7.92 (8.28)	4.59	252.84
2	2,2'-(1,4-phenylene)bis(ethan-1-aminium) $H_3N^+ \cdots NH_3^+$	-6.82	-0.52	10.54 8.69 (8.78)	4.10	281.77
3	3,3'-dimethoxy-[1,1-biphenyl]-4,4'-diaminium OCH_3 ... $H_3N^+ \cdots NH_3^+$ ... H_3CO	-6.75	-2.01	10.05 (9.94)	6.93	359.77
4	(1E,3E)-hexa-1,3,5-triene-1,6-diaminium $H_3N^+ \diagup\diagdown\diagup\diagdown NH_3^+$	-6.97	-2.54	8.75 (8.55)	5.11	202.82

[a]For systems [**1**]−[**4**]PbI$_4$, the N−N distance within the cations embedded in the perovskite (in parentheses) and the shortest interlayer I−I distance from the inorganic perovskite sublattice are also reported.
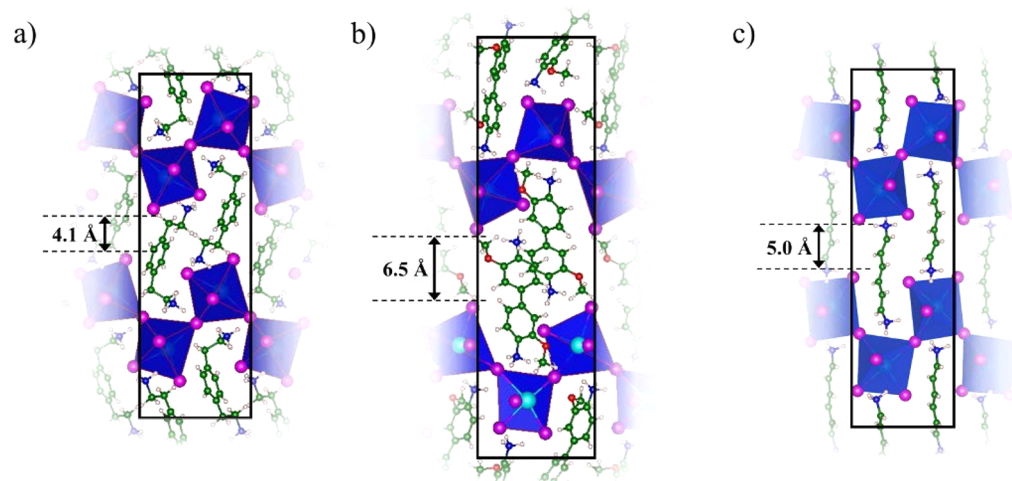
Figure 3. Optimized geometry structures of (a) [**2**]PbI$_4$, (b) [**3**]PbI$_4$, and (c) [**4**]PbI$_4$. The distance between the inorganic layers is also reported in angstroms.

and inorganic components, following the composite approach proposed by Traore et al.[27] We hence performed additional calculations for the separated inorganic sublattice lattice and organic spacers and realigned their corresponding PDOS with respect to deep electronic states of each moiety. As we see from Figure 2a, the aligned DOS of the isolated cations for EDBEPbI$_4$ has a sharp peak at approximately −2.8 eV, representing the HOMO of the isolated molecule. Upon interaction, EDBE states span ∼3 eV with a tail extending down to approximately −2 eV and a strongest contribution centered at −2.9 eV (Figure 2a). For NBT$_2$PbI$_4$ a reduced broadening of the organic cations states is calculated, despite the low-intensity tail spanning ∼3 eV. The contribution to cation states in this energy range comes from all the cation atoms with a slightly higher contribution from O and C atoms (see also the isodensity wave function plots of selected states in

Figure S1). Unoccupied cation states lie in both cases at much higher energy than the conduction band edge. The energetic spread of EDBE states over a large energy range and the significant broadening compared to the isolated molecule is consistent with an enhanced hole electronic coupling between the organic and inorganic moieties in EDBEPbI$_4$ than in NBT$_2$PbI$_4$, despite both EDBE and NBT being saturated organic cations. It is thus tempting to associate the enhanced coupling observed for EDBEPbI$_4$ to the (110) structural motif, which indeed implies a stronger interpenetration of the organic cations within the inorganic moiety (Figure 1a). Such enhanced interaction occurs because of the presence of unsaturated halide atoms at the inorganic−organic heterojunction, which also explains why the effect is less pronounced for electron carriers (with the CBE wave function contributed

mostly by Pb p orbitals, in contrast to VBE with large weights on I p orbitals).

Despite the somewhat surprising electronic coupling, the tailing of the VBE wave functions over the organic cations is still limited owing to an unfavorable starting organic/inorganic energy level alignment in EDBEPbI$_4$. To improve the energy alignment with respect to EDBE keeping the (110) structural motif we analyzed the electronic properties of a series of hypothetical dications (see Table 1 and Table S1 for the complete list of investigated structures). We also investigated several monocations (Table S2), which can serve as a useful data set for the design of novel (001) perovskites. We target molecules with a higher HOMO level than EDBE, required to optimize the energy level alignment between the inorganic and organic PDOS contributions at the VBE, and possibly a conjugated structure allowing vertical charge transfer. Our analysis is based on selecting new candidates considering three main features: (i) a steric encumbrance similar to EBDE, as quantified by the N−N distance between the terminal ammonium moieties; (ii) a more (less) positive HOMO (LUMO) energy level with respect to EDBE; and (iii) the presence of conjugated moieties to possibly favor charge delocalization and to increase the electronic coupling with the inorganic cage.

Considering this analysis, we selected molecules [2]−[4] in Table 1, which have dimensions similar to EDBE but show a more (less) positive energy level of HOMO (LUMO) and a partially conjugated moiety connecting the terminal ammonium groups. We thus adapted molecules [2]−[4] inside to the inorganic network of EDBEPbI$_4$, and we relaxed both ion position and cell parameters (see the resulting optimized structures in Figure 3).

By analyzing the DOS of the newly designed systems (see Figure 4), we find that there is a massive reorganization of the electronic structure when the organic cations are inserted into the inorganic layout in [2]PbI$_4$, [3]PbI$_4$, and [4]PbI$_4$. Most importantly, in contrast to EDBEPbI$_4$ (hereafter termed [1] PbI$_4$), the substantial electronic interactions between the closely spaced inorganic VB and organic HOMO prompt strong hybridization of the hole states, as exemplified by the large organic contribution to the DOS at the valence band edge (Figure 4). The resulting pinning of the occupied molecular orbitals is particularly striking in the case of [2]PbI$_4$, where peaks in the PDOS for the organic and inorganic components are perfectly superimposed. In addition, [3]PbI$_4$ shows quasi-degenerate organic cation states and perovskite conduction band edge, suggesting that the organic cation engineering could eventually lead to balanced electron/hole transfer across the inorganic layers. We stress that, in contrast to the situation prevailing for holes (where it is mostly driven by the electronic coupling between the organic and the inorganic layout), this resonance is accidental for electrons as a result of the much weaker wave function overlap with the lead orbitals; in the latter case, a close matching with the LUMO of the isolated molecule should thus be sought.

A summary of the energetic, structural, and electronic properties of the newly designed systems against the known [1]PbI$_4$ perovskite is reported in Table 2.

A fundamental parameter ruling whether a new perovskite will be likely formed from its precursors is the formation energy (ΔE in Table 2), defined here as the difference between the total energy of the perovskite minus that of the PbI$_2$, organic cations, and I$^-$ (see the Supporting Information).
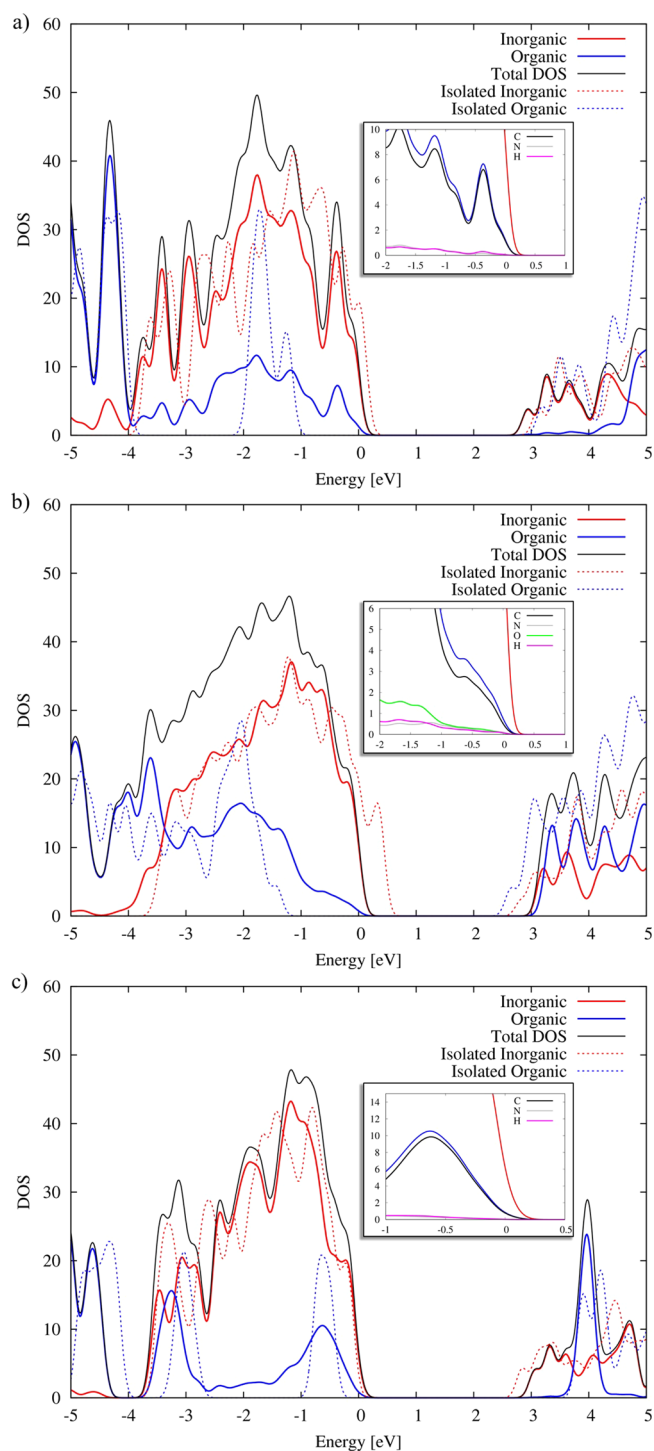
Figure 4. Partial density of states (PDOS) of (a) [2]PbI$_4$, (b) [3]PbI$_4$, and (c) [4]PbI$_4$. Red lines represent the inorganic part, and the blue lines represent the contribution of the organic cations. The full lines represent the PDOS of the complete system (organic and inorganic moieties interacting), and the dashed lines represent the DOS of organic and inorganic parts calculated separated.

Given this definition, the formation energies have relative relevance rather than absolute importance considering also that the vdW corrections are not included. As one may notice, [4]PbI$_4$ is predicted to have a more negative formation energy than the known [1]PbI$_4$ perovskite, suggesting that the former compound could have thermodynamic stability comparable to

Table 2. Calculated Formation Energies (ΔE, eV), Band Gap (eV, HSE06-SOC), Calculated Cell Parameters (a-b-c, Å), Average Distance between the Inorganic Layers (d, Å), and Effective Masses Calculated along the Direction in Reciprocal Space Corresponding to the b Crystal Axis[a]

	ΔE	band gap	$a/b/c$	d	m_{h}	m_{e}
[1]PbI$_4$	−7.87	2.84	6.5/29.3/9.3	4.6	3.33	4.33
[2]PbI$_4$	−7.19	2.92	6.2/28.0/8.8	4.1	2.46	2.43
[3]PbI$_4$	−4.92	3.15	6.7/32.7/9.3	6.5		
[4]PbI$_4$	−8.52	3.04	6.3/30.0/8.9	5.0	1.78	2.20

[a]Y → C (PBE-SOC), see also calculated band structures in the Supporting Information.

the prototype [1]PbI$_4$ perovskite. [3]PbI4 shows a significantly lower ΔE than [1]PbI4, implying a somewhat reduced chance of forming stable compounds for this newly proposed perovskite, while [2]PbI4 has an intermediate ΔE. The significantly lower ΔE value calculated for [3]PbI4 is related to the significant structural distortion introduced by these new cations into the perovskite lattice, which can be quantified by the variation of the cell parameters compared to [1]PbI$_4$ (Table 2) and by global distortion parameters such as the deviation from the ideal angle for each octahedra and their average (see Table S3). Such structural distortions affect not only the formation energy but also the band gap of the investigated systems, with [3]PbI$_4$ showing a 0.3 eV higher bandgap than [1]PbI$_4$. This finding is in line with earlier reports of the relationships between structural deformations and bandgap evolution in perovskites.[10,28] Previous studies also showed that structural distortion, in particular octahedra tilting, also affected the transport properties of metal halide perovskites, with higher effective masses predicted for more distorted perovskites.[28] Looking at the data in Table 2 we see that [2]PbI$_4$ has higher band gap than the prototype [1]PbI$_4$ compound, but it also features lower electron/hole effective masses for vertical transport. For [3]PbI$_4$ we obtain no dispersion along the stacking direction, implying an infinite effective mass, while [4]PbI$_4$ shows the lowest calculated effective masses. Notice that such effective masses for the out-of-plane direction of these 2D perovskites are about 1 order of magnitude greater than those found for typical 3D lead iodide compounds.[29] This is expected in light of the spacing introduced between the inorganic layers which reduces the overlap across the different layers. The whole band structure for the investigated systems is reported in Figure S4.

Notably, there appears to be some correlation between the spacing parameter (d in Table 2) and the carrier effective masses, which is tuned by the cation dimension (see also model calculations in the Supporting Information, Figure S3 and Table S4). However, this is not the only parameter to be considered, as for [4]PbI$_4$ we predict an increased spacing but reduced carrier effective masses, compared to e.g. [1]PbI$_4$, implying that the new energy-tuned cation [4], with electronic states contributing to the VBE and conjugated organic structure, effectively modulates vertical transport. In addition to structural and electronic properties, it is worth mentioning that introducing more rigid aromatic cation spacers may lead to reduced electron−phonon coupling and consequently increase the lifetime of photogenerated carriers in 2D perovskites.[30] Although we have not quantitatively assessed the impact of such behavior in the selected compounds, we anticipate that replacing EDBE alkyl chains with aromatic or

conjugated moieties in structure [2−4] PbI$_4$ could have a similar beneficial impact on carrier dynamics.

In summary, our analysis shows that cation engineering has an important role in optimizing the transport properties in 2D perovskites. By performing computational analyses on energy and sterically selected organic cations we were able to rationalize the two main roles of the organic cations in low-dimensional perovskite: (i) the electronic properties of the organic cation has an effect on the charge transport; (ii) the structure of the cation, and mainly his size, allows us to tune the distance between the inorganic layers, which results in a significant change of the electronic and charge transport properties of the material. We find, in particular, that tuning the energy alignment between the HOMO and LUMO level of the organic cation on the energy of the band edges of the inorganic part of the material should increase the charge hopping efficiency; the tuning of the interlayer distance by the chemical structure and encumbrance of the cation is an even more important parameter to take into account to obtain satisfying electronic and charge transport properties in the two-dimensional perovskite materials. Indeed, we showed that the electron and hole effective masses calculated along the stacking direction are directly correlated to the distance between the inorganic layers. However, even more important, thanks to our latest results, we showed that there is a balance to find between these two main roles. The overall picture extracted from this work can be useful to draw the guidelines for the design of high performing solar cells based on 2D lead halide perovskites, and the next step of this study would be to apply this systematic methodology to actual experimental structures.

■ ASSOCIATED CONTENT

ⓢ Supporting Information

The Supporting Information is available free of charge at https://pubs.acs.org/doi/10.1021/acs.jpclett.0c03843.

> Full data set of the investigated cations, effective masses, geometrical distortion parameters and computational details (PDF)

■ AUTHOR INFORMATION

Corresponding Authors

Edoardo Mosconi − *Computational Laboratory for Hybrid/Organic Photovoltaics (CLHYO), Istituto CNR di Scienze e Tecnologie Chimiche "Giulio Natta" (CNR-SCITEC), 06123 Perugia, Italy;* ⓞ orcid.org/0000-0001-5075-6664; Email: edoardo@thch.unipg.it

Filippo De Angelis − *Computational Laboratory for Hybrid/Organic Photovoltaics (CLHYO), Istituto CNR di Scienze e Tecnologie Chimiche "Giulio Natta" (CNR-SCITEC), 06123 Perugia, Italy; CompuNet, Istituto Italiano di Tecnologia, 16163 Genova, Italy; Department of Chemistry, Biology and Biotechnology, University of Perugia, 06123 Perugia, Italy;* ⓞ orcid.org/0000-0003-3833-1975; Email: filippo@thch.unipg.it

Authors

Nadège Marchal − *Computational Laboratory for Hybrid/Organic Photovoltaics (CLHYO), Istituto CNR di Scienze e Tecnologie Chimiche "Giulio Natta" (CNR-SCITEC), 06123 Perugia, Italy; Laboratory for Chemistry of Novel Materials, University of Mons, B-7000 Mons, Belgium*

Gonzalo García-Espejo — *Departamento de Química Física, Instituto Universitario de Investigación en Química Fina y Nanoquímica, IUQFN, Universidad de Córdoba, E-14071 Córdoba, Spain*

Tahani M. Almutairi — *Chemistry Department, College of Science, King Saud University, Riyadh 11451, Saudi Arabia*

Claudio Quarti — *Laboratory for Chemistry of Novel Materials, University of Mons, B-7000 Mons, Belgium;* orcid.org/0000-0002-5488-1216

David Beljonne — *Laboratory for Chemistry of Novel Materials, University of Mons, B-7000 Mons, Belgium;* orcid.org/0000-0002-2989-3557

Complete contact information is available at:
https://pubs.acs.org/10.1021/acs.jpclett.0c03843

Notes

The authors declare no competing financial interest.

REFERENCES

(1) Stranks, S. D.; Snaith, H. J. Metal-halide perovskites for photovoltaic and light-emitting devices. *Nat. Nanotechnol.* **2015**, *10*, 391−402.

(2) Kojima, A.; Teshima, K.; Shirai, Y.; Miyasaka, T. Organometal Halide Perovskites as Visible-Light Sensitizers for Photovoltaic Cells. *J. Am. Chem. Soc.* **2009**, *131*, 6050−6051.

(3) Im, J.-H.; Lee, C.-R.; Lee, J.-W.; Park, S.-W.; Park, N.-G. 6.5% efficient perovskite quantum-dot-sensitized solar cell. *Nanoscale* **2011**, *3*, 4088−4093.

(4) Liu, M.; Johnston, M. B.; Snaith, H. J. Efficient Planar Heterojunction Perovskite Solar Cells by Vapour Deposition. *Nature* **2013**, *501*, 395−398.

(5) Burschka, J.; Pellet, N.; Moon, S.-J.; Humphry-Baker, R.; Gao, P.; Nazeeruddin, M. K.; Grätzel, M. Sequential deposition as a route to high-performance perovskite-sensitized solar cells. *Nature* **2013**, *499*, 316−319.

(6) Zhou, H.; Chen, Q.; Li, G.; Luo, S.; Song, T.-B.; Duan, H.-S.; Hong, Z.; You, J.; Liu, Y.; Yang, Y. Interface engineering of highly efficient perovskite solar cells. *Science* **2014**, *345*, 542−546.

(7) Jeon, N. J.; Noh, J. H.; Yang, W. S.; Kim, Y. C.; Ryu, S.; Seo, J.; Seok, S. I. Compositional Engineering of Perovskite Materials for High-Performance Solar Cells. *Nature* **2015**, *517*, 476−480.

(8) National Renewable Energy Laboratory. Efficiency chart (2021). https://www.nrel.gov/pv/cell-efficiency.html.

(9) Meng, L.; You, J.; Yang, Y. Addressing the stability issue of perovskite solar cells for commercial applications. *Nat. Commun.* **2018**, *9*, 5265.

(10) Amat, A.; Mosconi, E.; Ronca, E.; Quarti, C.; Umari, P.; Nazeeruddin, M. K.; Grätzel, M.; De Angelis, F. Cation-Induced Band-Gap Tuning in Organohalide Perovskites: Interplay of Spin-Orbit Coupling and Octahedra Tilting. *Nano Lett.* **2014**, *14*, 3608−3616.

(11) Even, J.; Pedesseau, L.; Katan, C. Understanding Quantum Confinement of Charge Carriers in Layered 2D Hybrid Perovskites. *ChemPhysChem* **2014**, *15*, 3733−3741.

(12) Sapori, D.; Kepenekian, M.; Pedesseau, L.; Katan, C.; Even, J. Quantum Confinement and Dielectric Profiles of Colloidal Nanoplatelets of Halide Inorganic and Hybrid Organic-Inorganic Perovskites. *Nanoscale* **2016**, *8*, 6369−6378.

(13) Katan, C.; Mercier, N.; Even, J. Quantum and Dielectric Confinement Effects in Lower-Dimensional Hybrid Perovskite Semiconductors. *Chem. Rev.* **2019**, *119*, 3140−3192.

(14) Quarti, C.; Marchal, N.; Beljonne, D. Tuning the Optoelectronic Properties of Two-Dimensional Hybrid Perovskite Semiconductors with Alkyl Chain Spacers. *J. Phys. Chem. Lett.* **2018**, *9*, 3416−3424.

(15) Gan, L.; Li, J.; Fang, Z.; He, H.; Ye, Z. Effects of Organic Cation Length on Exciton Recombination in Two-Dimensional Layered Lead Iodide Hybrid Perovskite Crystals. *J. Phys. Chem. Lett.* **2017**, *8*, 5177−5183.

(16) Grancini, G.; Roldán-Carmona, C.; Zimmermann, I.; Mosconi, E.; Lee, X.; Martineau, D.; Narbey, S.; Oswald, F.; De Angelis, F.; Graetzel, M.; Nazeeruddin, M. K. One-Year stable perovskite solar cells by 2D/3D interface engineering. *Nat. Commun.* **2017**, *8*, 15684.

(17) Krishna, A.; Gottis, S.; Nazeeruddin, M. K.; Sauvage, F. Mixed Dimensional 2D/3D Hybrid Perovskite Absorbers: The Future of Perovskite Solar Cells? *Adv. Funct. Mater.* **2019**, *29*, 1806482.

(18) Zhang, F.; Kim, D. H.; Zhu, K. 3D/2D multidimensional perovskites: Balance of high performance and stability for perovskite solar cells. *Curr. Opin. Electrochem.* **2018**, *11*, 105−113.

(19) Tsai, H.; Nie, W.; Blancon, J.-C.; Stoumpos, C. C.; Asadpour, R.; Harutyunyan, B.; Neukirch, A. J.; Verduzco, R.; Crochet, J. J.; Tretiak, S.; et al. High-efficiency two-dimensional Ruddlesden-Popper perovskite solar cells. *Nature* **2016**, *536*, 312.

(20) Maheshwari, S.; Savenije, T. J.; Renaud, N.; Grozema, F. C. Computational Design of Two-Dimensional Perovskites with Functional Organic Cations. *J. Phys. Chem. C* **2018**, *122*, 17118−17122.

(21) Mitzi, D. B. Solution-processed inorganic semiconductors. *J. Mater. Chem.* **2004**, *14*, 2355−2365.

(22) Mitzi, D. B. Templating and structural engineering in organic-inorganic perovskites. *J. Chem. Soc., Dalton Trans.* **2001**, *1*, 1−12.

(23) Mitzi, D. B.; Chondroudis, K.; Kagan, C. R. Design, Structure, and Optical Properties of Organic-Inorganic Perovskites Containing an Oligothiophene Chromophore. *Inorg. Chem.* **1999**, *38*, 6246−6256.

(24) Van Gompel, W. T. M.; Herckens, R.; Van Hecke, K.; Ruttens, B.; D'Haen, J.; Lutsen, L.; Vanderzande, D. Towards 2D layered hybrid perovskites with enhanced functionality: introducing charge-transfer complexes via self-assembly. *ChemComm* **2019**, *55*, 2481−2484.

(25) Cortecchia, D.; Neutzner, S.; Srimath Kandada, A. R.; Mosconi, E.; Meggiolaro, D.; De Angelis, F.; Soci, C.; Petrozza, A. Broadband Emission in Two-Dimensional Hybrid Perovskites: The Role of Structural Deformation. *J. Am. Chem. Soc.* **2017**, *139*, 39−42.

(26) Muscat, J. P.; Newns, D. M. Chemisorption on metals. *Prog. Surf. Sci.* **1978**, *9*, 1−43.

(27) Traore, B.; Pedesseau, L.; Assam, L.; Che, X.; Blancon, J.-C.; Tsai, H.; Nie, W.; Stoumpos, C. C.; Kanatzidis, M. G.; Tretiak, S.; et al. Composite Nature of Layered Hybrid Perovskites: Assessment on Quantum and Dielectric Confinements and Band Alignment. *ACS Nano* **2018**, *12*, 3321−3332.

(28) Knutson, J. L.; Martin, J. D.; Mitzi, D. B. Tuning the Band Gap in Hybrid Tin Iodide Perovskite Semiconductors Using Structural Templating. *Inorg. Chem.* **2005**, *44*, 4699−4705.

(29) Giorgi, G.; Fujisawa, J.-I.; Segawa, H.; Yamashita, K. Small Photocarrier Effective Masses Featuring Ambipolar Transport in Methylammonium Lead Iodide Perovskite: A Density Functional Analysis. *J. Phys. Chem. Lett.* **2013**, *4*, 4213−4216.

(30) Gong, X.; Voznyy, O.; Jain, A.; Liu, W.; Sabatini, R.; Piontkowski, Z.; Walters, G.; Bappi, G.; Nokhrin, S.; Bushuyev, O.; et al. Electron-phonon interaction in efficient perovskite blue emitters. *Nat. Mater.* **2018**, *17*, 550−556.